

Mass and energy distributions of fusion products from ^{32}S on ^{12}C , ^{25}Mg , and $^{40}\text{Ca}^\dagger$

J. D. Garrett and H. E. Wegner

Brookhaven National Laboratory, Upton, New York 11973

T. M. Cormier, E. R. Cosman, and A. J. Lazzarini

*Physics Department and Laboratory for Nuclear Structure,
Massachusetts Institute of Technology, Cambridge, Massachusetts 02139*

(Received 3 April 1975)

The mass and energy distributions for fusion products corresponding to 128.9 MeV ^{32}S on ^{12}C , ^{25}Mg , and ^{40}Ca targets has been measured at 8° lab using a time-of-flight spectrometer. The heaviest product observed with significant cross section for each system has a mass five units less than that of the corresponding compound system. Lighter dominant mass groups are separated by approximately three mass units. Such mass systematics can be understood in terms of neutron, proton, and α -particle competition in the deexcitation of the compound system and are reproduced qualitatively by particle evaporation calculations.

[NUCLEAR REACTIONS $^{32}\text{S} + ^{12}\text{C}$, ^{25}Mg , ^{40}Ca fusion, $E = 128.9$ MeV; measured
mass and energy distribution of products.]

I. INTRODUCTION

The advent of more energetic heavy ion beams from newly upgraded tandem accelerators allows the fusion of two heavy systems to be studied. Fusion cross sections have been measured for a variety of beams and targets (see e.g. Refs. 1-7). In most cases, however, the mass resolution has not been sufficient to determine the fusion product mass distribution.⁸ The recent development of a fast time-of-flight system⁹ at the Brookhaven National Laboratory tandem accelerator facility allows fusion products to be studied with a mass resolution of approximately 1 mass unit in 50. This system, coupled with the multiparticle acceleration capability (for calibration purposes) allows a precise mass and energy determination for a large dynamic range of reaction and fusion products.

The present paper reports measurements of the mass distributions for fusion products at an 8° lab scattering angle formed by 128.9 MeV ^{32}S ions incident on ^{12}C , ^{25}Mg , and ^{40}Ca targets. For all targets a strikingly similar mass dependence was observed. The heaviest fusion product observed to be populated with a large yield has a mass five units less than that of the compound system. Large cross sections also were observed for lighter mass groups separated by three mass units. Such mass systematics for the fusion products can be understood in terms of neutron, proton, and α particle competition in the deexcitation of the compound nucleus, and indeed, are reproduced qualitatively by particle evaporation calculations.

II. EXPERIMENTAL PROCEDURES

A 128.9 MeV ^{32}S beam from the Brookhaven National Laboratory tandem accelerator facility was used to study the mass distribution of the fusion products at an 8° lab scattering angle from a self-supporting natural C target ($\sim 35 \mu\text{g}/\text{cm}^2$) and from C backed ^{25}Mg ($>95\%$ enrichment) and natural Ca (96.9% ^{40}Ca) targets of $\approx 100 \mu\text{g}/\text{cm}^2$ areal density. The time-of-flight arrangement for the measurement of the fusion product masses was similar to that described previously.⁹ Briefly, fusion products exiting from the target in a small sliding window target chamber pass through an $\approx 200 \mu\text{g}/\text{cm}^2$ Pilot B¹⁰ scintillator foil providing a start signal. After traveling approximately 2 m beyond the scintillator, they are stopped in a 300 mm² silicon diode detector which provides the stop pulse as well as the E signal for each detected event. The time-of-flight spectrometer had a solid angle of ≈ 0.04 msr and an angular resolution $\approx \pm 0.2^\circ$ lab.

Two analog multiplier circuits were used to square the time signal T and multiply it by the energy signal E to form the product ET^2 which is proportional to the fragment mass. The mass signal was then displayed on a 256 channel array in correlation with the E signal on a 128 channel array.

A typical variable density computer plot of the calcium fusion data measured at an incident energy of 128.9 MeV and at a laboratory angle of 8° is shown in Fig. 1. The data points forming the intense vertical line on the left represent ^{32}S ions

of all energies scattered from the target. The intense peak at the upper extreme is the elastic group. The parallel lines corresponding to higher mass groups close to the sulfur mass line are fusion products formed from the carbon backing and oxygen impurities in the calcium target. The three clustered mass groups to the right are products from $^{32}\text{S} + ^{40}\text{Ca}$ fusion.

The E - ET^2 matrix was calibrated by scattering ^{45}Sc , ^{51}V , ^{58}Ni , ^{64}Zn , and ^{74}Ge ions from a $75 \mu\text{g}/\text{cm}^2$ Au target at 3° lab. These different mass beams form vertical mass lines similar to that observed for sulfur and provide a characteristic "signature" of a given mass particle over a wide energy range in different mass regions. Some of the heavier mass ions also were accelerated at several different energies ranging from 30 to 100 MeV. The corresponding strong elastic peaks allow an accurate energy scale to be established for each of the calibrated mass regions. Since both the mass and energy responses are not linear over the entire dynamic range of the products, it is important that such a mass-energy calibration be

established. At the beginning of the experimental period the elastic scattering calibration was made using all of the different ions at a variety of incident energies. Such a procedure took only a few hours using the sputter ion source.¹¹ After the fusion data were accumulated, the calibration was checked using the ^{51}V beam.

III. DATA ANALYSIS

The data were analyzed by taking Y (energy) cuts through the different mass groups along the X (mass) axis. A cut in the X direction through the mass 32 line gives a peak that can be reproduced by a Gaussian shape establishing the centroid for that mass group accurate to ≈ 0.1 channel. The centroids and widths of the mass lines corresponding to elastic scattering (see e.g. Fig. 2) characterize a single mass line as provided by the accelerated ions after transiting the detection system. Cuts through the fusion region show a series of peaks which can be reproduced by a Gaussian shape. In the case of the fusion products, all of

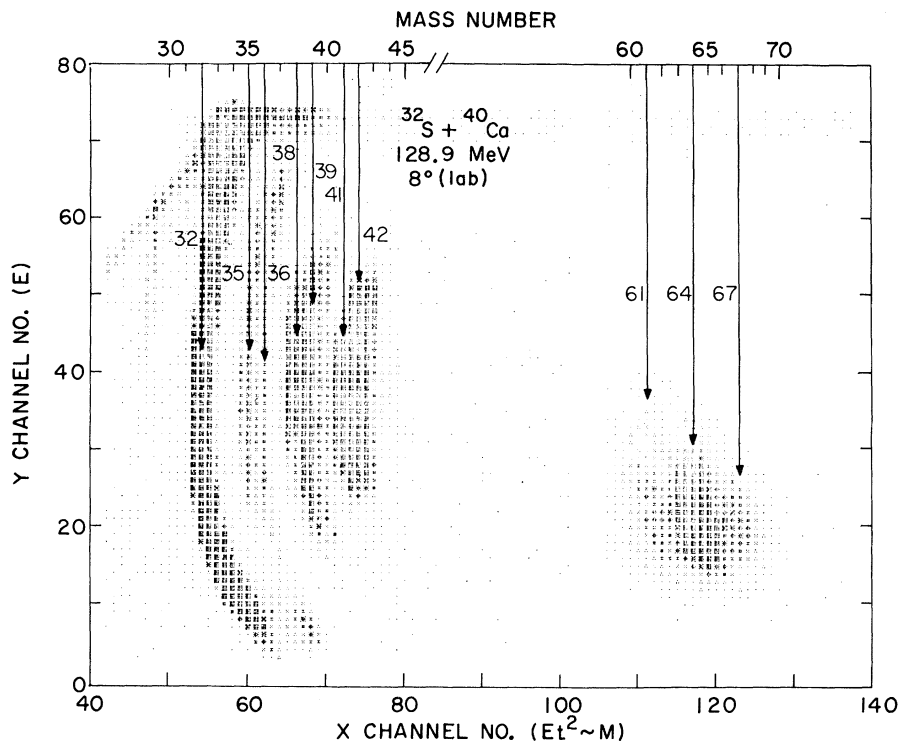


FIG. 1. Variable density plot of a portion of the 256×128 channel spectrum for the reaction; $128.9 \text{ MeV } ^{32}\text{S} + ^{40}\text{Ca}$, 8° lab. The plotted points of variable size correspond to a channel count range of 10 with the solid square corresponding to ≥ 50 counts. The intense elastic ^{32}S peak near (57, 70) in the upper left-hand corner defines the upper end of the loci of data points that comprise the mass 32 line which extends down to the electronic cutoff region. Fusion with light target contaminants and transfer reactions result in other similarly shaped mass lines near mass 32. The points on the right are the fusion products from the reaction $^{32}\text{S} + ^{40}\text{Ca}$. The three dominant mass lines (see Fig. 2) are labeled. The mass lines are curved because of nonlinearities in the over-all response of the system.

the fit parameters were allowed to vary with the restraint that the width of all peaks were the same.

IV. EXPERIMENTAL DATA

A. $^{32}\text{S} + ^{40}\text{Ca}$ fusion

Figure 2 summarizes the results of such an analysis for the fusion products formed by 128.9 MeV ^{32}S ions on ^{40}Ca . For comparison, a mass line corresponding to elastically scattered ^{64}Zn is superimposed on the fusion data showing the characteristic shape of a typical mass line. The mass calibration was determined using this line and similar lines from ^{74}Ge and ^{58}Ni scattering not shown in the figure. A typical mass spectra at constant energy (corresponding to Y equals channel 22 and indicated by a dashed line) through the fusion region also is shown at the top of Fig. 2. The solid line in the mass spectra corresponds to

the best three peak fit to the data, while the dashed line shows three peaks with the width of a single mass line as determined from a fit to the scattered ^{64}Zn line. Since the fitted peaks are $\sim 20\%$ wider than those fitted to the ^{64}Zn mass line, additional adjacent masses must contribute to the width of the fusion groups. The location of the fitted peak indicates which predominant mass is involved in that particular cut and what influence other masses have at that energy. A strong central peak will tend to force the fitted width of the weaker peaks; however, the consistency of the centroid location indicates that certain masses are predominately involved in the fusion product.

The strong peak in the $^{32}\text{S} + ^{40}\text{Ca}$ data follows the mass 64 line although it is slightly shifted toward higher masses indicating that mass 65 products are important in the fusion process as well although they are not resolved. The mass 67 and 61 centroids are less consistent; however, it still

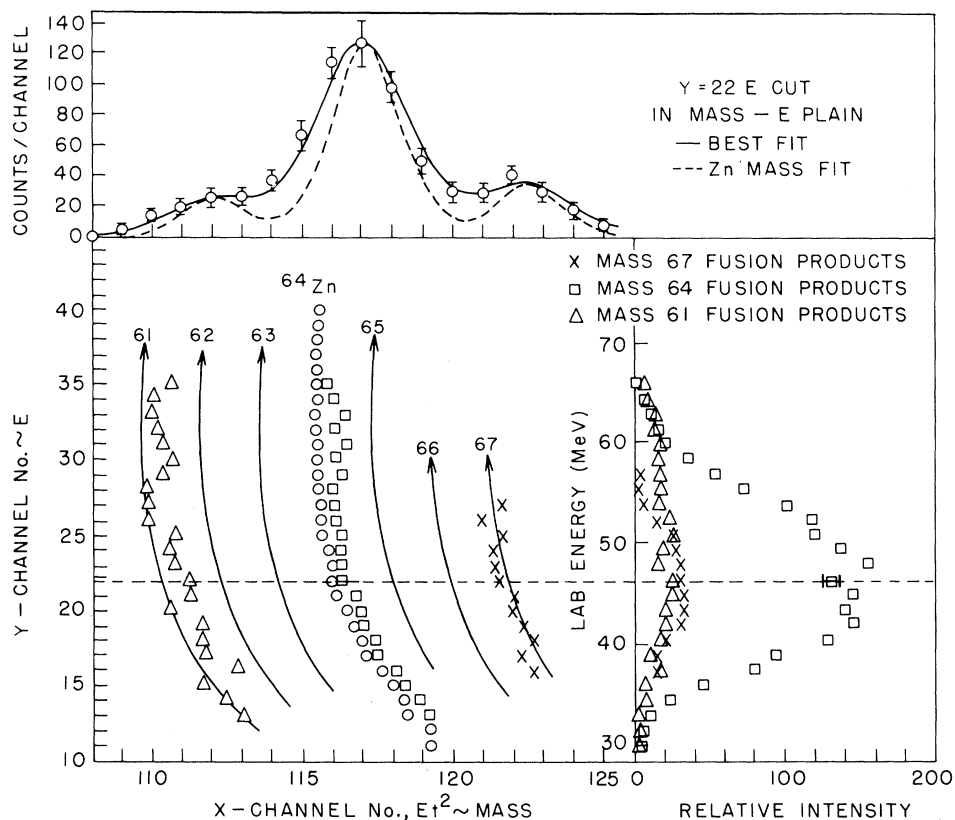


FIG. 2. Results of a computer analysis of the fusion product region of Fig. 1. The open circle points superimposed on the fusion data points correspond to centroid locations determined by a fit to a mass line obtained by scattering ^{64}Zn from a Au target. The mass calibration was obtained using the ^{64}Zn line and other scattered heavy ions not shown in this figure. A cut through the fusion region at $Y=22$, corresponding to a fusion product energy of approximately 46 MeV, is shown in the upper part of the figure with its corresponding best fit. The single mass resolution of the system for mass 64 is shown at the fusion mass centroid locations for comparison. The relative energy dependence for the different mass groups is indicated on the right.

can be concluded from the peak locations that the dominant masses of these groups are 67 and 61. The relative intensity as a function of energy for each of these three mass lines is displayed on the right in Fig. 2.

In summary, the fusion products from 128.9 MeV ^{32}S and ^{40}Ca at 8° lab range in laboratory energy from 30 to 65 MeV. Masses 67, 64, and 61 have the largest fusion cross sections with intermediate masses accounting for 10 to 20% of the dominant mass group, $A = 64$.

B. $^{32}\text{S} + ^{25}\text{Mg}$ fusion

The results of the analysis of the fusion of 128.9 MeV ^{32}S ions with ^{25}Mg at 8° lab are shown in Fig. 3. Both the elastically scattered ^{45}Sc and ^{51}V mass lines are superimposed in order to show the characteristic "signature" of a single mass group. The layout of this figure is similar to that described above for the ^{40}Ca data shown in Fig. 2. The mass 52 and 47 fusion groups follow the respective mass lines quite well; however, the centroid of the mass

group corresponding to the largest cross section varies between mass 49 and mass 50. This group is considerably wider than the reference mass groups suggesting that two masses contribute. There also are indications from the inconsistent centroid location of the fitted peak that the intensity of the masses contributing to this group varies as a function of particle energy. Similarly, a weak group scatters about mass 44 over most of its energy range but tends towards mass 43 at the highest fusion energies. In this case, the energies of the fusion fragments range from 25 to 90 MeV in the extreme with a mean energy around 58 MeV corresponding to the displayed Y cut. Appreciable contributions are observed corresponding to masses between the fitted mass groups. It would appear that these intermediate groups are more important than in the case of ^{40}Ca ; however, this may be only an artifact of the better mass resolution for the lighter $^{32}\text{S} + ^{25}\text{Mg}$ fusion products.

In summary, the fusion products from 128.9 MeV ^{32}S on ^{25}Mg at 8° lab range from 25 to 90 MeV lab-

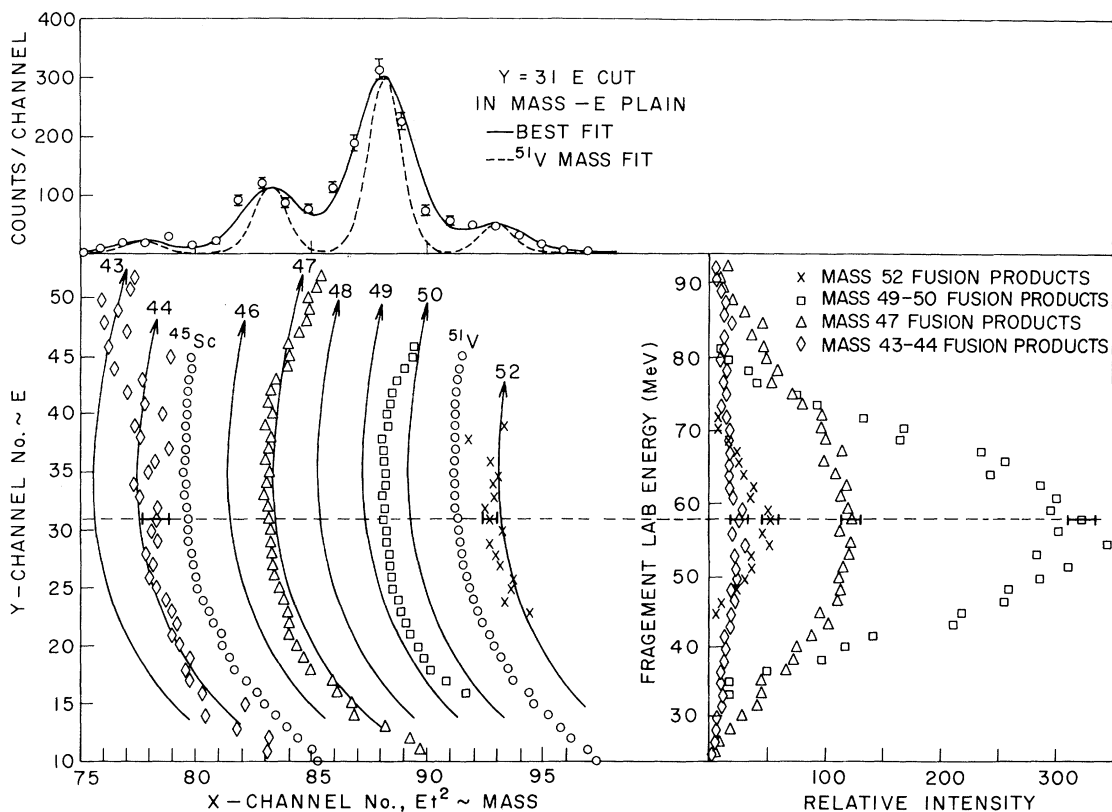


FIG. 3. Results of a computer analysis for fusion data similar to that of Fig. 1 for the reaction; 128.9 MeV $^{32}\text{S} + ^{25}\text{Mg}$, 8° lab. The two open circle data groups labeled ^{45}Sc and ^{51}V correspond to the centroid locations determined by fits to calibration mass lines produced by ^{45}Sc and ^{51}V beams. The mass calibration lines are determined from the ^{45}Sc and ^{51}V lines as well as other calibration lines not shown. The fusion products from this reaction are represented by the other data points as indicated for various mass regions.

oratory energy. The largest cross sections are observed for masses 52, 49-50, 47, and 43-44. Apparently both masses 49 and 50 contribute to the mass group with the largest fusion cross section at this incident energy and angle.

C. $^{32}\text{S}+^{12}\text{C}$ fusion

The results of the analysis of the fusion of 128.9 MeV ^{32}S ions with ^{12}C at 8° lab are shown in Fig. 4. The superior resolution of this lighter mass data allows the individual mass groups to be fitted with the line width of the ^{32}S mass line. A five peak analysis was used, and although there are relatively few data points to describe or locate different peaks, the fits for the five peaks was remarkably consistent. A typical cut through $Y = 45$ (corresponding to a fusion particle energy of ~ 78 MeV) is displayed.

The fusion products range in energy from ~ 40 to 110 MeV. The $A = 38$ and 39 mass groups have the largest fusion cross sections at this angle.

Two additional mass groups are observed at $A = 35$ and 36. These doublets are consistent with the suggestion that the dominant mass group observed for $^{32}\text{S} + ^{25}\text{Mg}$ fusion also contains contributions from two masses (see Sec. IV B). The mass 3 separation between strongly populated fusion products remains in the better resolution ^{12}C data. The low energy data depart completely from the characteristic mass shape as defined by the ^{32}S mass line (also shown in Fig. 4) indicating that other masses contribute when large amounts of energy are lost by the fragments.

V. DISCUSSION

The dominant masses of the fusion products at 8° lab determined from the data discussed in Sec. IV are summarized in Table I. For each system studied the heaviest fusion product observed to be formed with a large cross section has a mass five units less than the corresponding compound system. Lighter dominant mass groups are separated

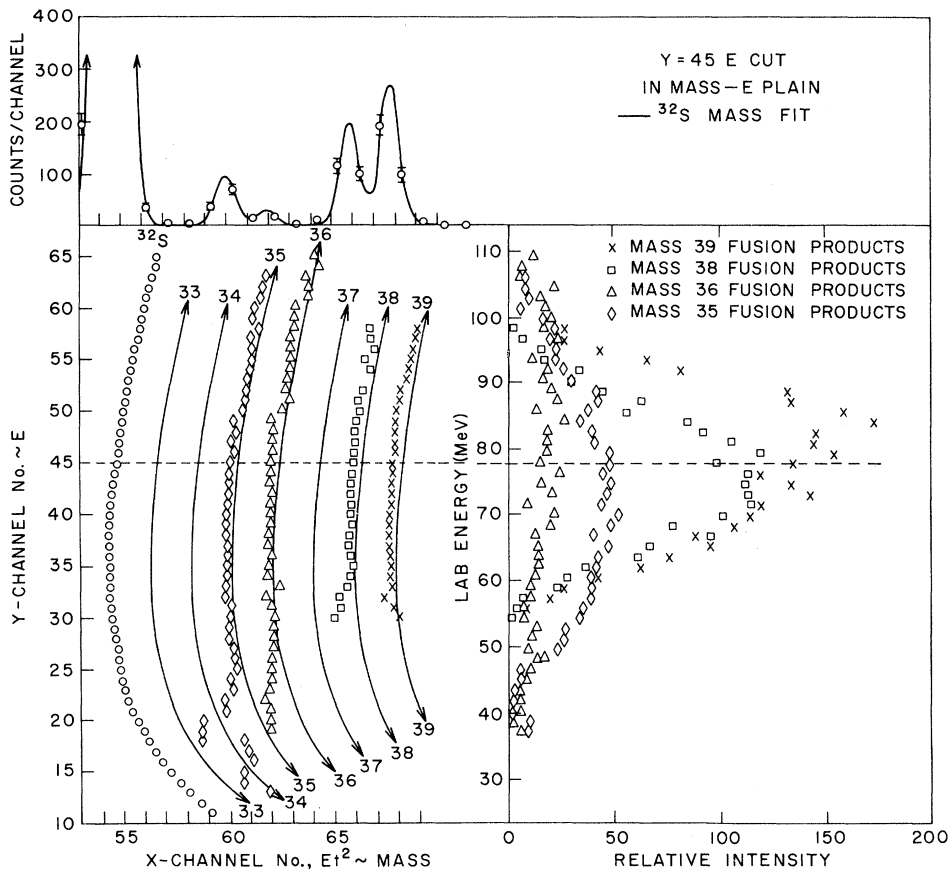


FIG. 4. Results of a computer analysis for the fusion mass lines close to the ^{32}S mass line in Fig. 1 corresponding to the reaction; 128.9 MeV $^{32}\text{S} + ^{12}\text{C}$, 8° lab. In this case the beam providing the fusion reaction is one of the calibration mass lines.

TABLE I. Summary of fusion reactions studied.

Target	Compound system	$E_{c.m.} (^{32}\text{S})^a$ (MeV)	Q value ^b (MeV)	Compound system E_x (MeV)	Dominant ^c masses
^{12}C	^{44}Ti	35.15	11.53	46.68	35, 36, 38, 39
^{25}Mg	^{57}Ni	56.54	16.90	73.44	43-44, 47, 49-50, 52
^{40}Ca	^{72}Kr	71.61	-4.4 ^d	67.2 ^d	61, 64, 67

^a Corresponds to lab energy of 128.9 MeV ^{32}S .

^b Binding energy difference between compound nucleus and ^{32}S plus target.

^c Dominant masses of fusion products at 8° lab. See Sec. IV and Figs. 2-4.

^d Based on masses calculated using Meyers-Swiatecki-Lysekil mass formula.

by approximately three mass units. Preliminary data¹² at other scattering angles indicate that the mass three separation for the dominant masses of fusion products is independent of angle.

The observed fusion product mass systematics can be understood in terms of competition between multiple neutron, proton, and α -particle emission in the deexcitation of a compound system at high excitation energies. The heaviest group of fusion products correspond to multiple nucleon emission. The difference in excitation energies of the ^{57}Ni (fused $^{32}\text{S} + ^{25}\text{Mg}$) and the ^{72}Kr (fused $^{32}\text{S} + ^{40}\text{Ca}$) compound systems studied is small (≈ 6 MeV out of ≈ 70 MeV). Therefore, on the average, about the same number of nucleons should be emitted from these two systems if the neutron and proton binding energies are similar in the two decay chains (see Table II). Indeed, the heaviest fusion product observed for both ^{25}Mg and the ^{40}Ca targets has a mass five units less than that of the corresponding compound system.¹³ The lighter mass groups of fusion products correspond to α emission plus multiple nucleon emission. When an α particle is emitted, sufficient energy is lost so that on the average one less nucleon decay can take place. Thus the resulting masses of the most abundant fusion products from x nucleon; α, x nucleon; and $2\alpha, x$ nucleon decay are separated by three mass units. Such systematics would be obtained if at each stage in the deexcitation process nearly the

same excitation energy is removed from the system in neutron, proton, and α -particle emission. Less kinetic energy is associated with neutron decay than either proton or α -particle decay because there is no Coulomb barrier for the neutron channel. The nuclei in the decay chains studied, however, are neutron deficient; therefore, the neutron thresholds are higher than either the proton or α -particle thresholds (see Table II). Thus protons and α particles remove nearly the same excitation energy from the decaying system as the neutron emission.

Similar enhanced cross sections for fusion products differing by about three mass units might be expected in other fusion studies leading to neutron deficient compound systems. Indeed a separation of three mass units is observed between the maximum α, x nucleon and x nucleon cross sections following the fusion of ^{16}O with $^{58,60,61}\text{Ni}$ (Ref. 6) and C and O fusion with rare earth nuclei.⁷

The observed mass systematics of the differential cross section is reproduced qualitatively by the total cross section using the compound nucleus deexcitation code ALICE,¹⁴ which includes competition between neutron, proton, and α -particle emission, calculated using the statistical formalism of Weisskopf and Ewing.¹⁵ The predicted $^{32}\text{S} + ^{40}\text{Ca}$ fusion cross section as a function of the product mass is shown in the top portion of Fig. 5. As observed (see Fig. 2), the largest cross sections are

TABLE II. Average and range of binding energies for daughters of $^{32}\text{S} + ^{25}\text{Mg}$ and ^{40}Ca .

Decay products	$^{32}\text{S} + ^{25}\text{Mg}$		$^{32}\text{S} + ^{40}\text{Ca}$	
	Av. B.E. ^a (MeV)	B.E. range ^a (MeV)	Av. B.E. ^a (MeV)	B.E. range ^a (MeV)
n	14.9	11.3-19.1	14.4	12.1-19.9
p	4.2	-0.1- 6.9	1.0	-2.6- 5.3
α	8.2	7.0- 9.5	2.3	0.1- 9.3

^a Binding energies (B.E.) calculated using the Myers-Swiatecki-Lysekil mass formula for daughters having up to nine nucleons less than the compound nucleus.

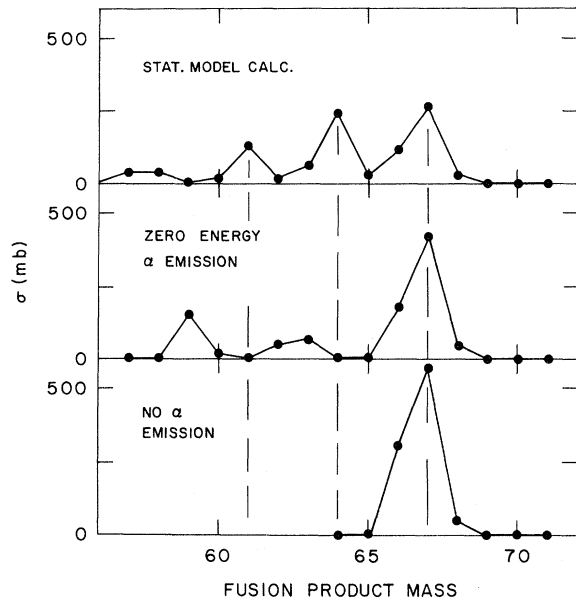


FIG. 5. Predicted total cross sections as a function of the fusion product mass for the deexcitation of fused 128.9 MeV ^{32}S on ^{40}Ca . The top portion of the figure shows the standard ALICE calculation which includes competition between n , p , and α emission. The predicted enhanced yield of products for $A = 61$, 64 , and 67 is observed in the experimental data measured at 8° lab angle (see Fig. 2); however, the details of the relative yield for the different masses at the angle measured are not completely reproduced. The middle portion of the figure shows similar calculations except that the excitation energy of the system is not reduced for α emission. The predicted mass three systematics for the yield of fusion products changes for this nonphysical calculation. The enhanced yield for the lighter mass products move to lower masses producing large cross sections for masses separated by four mass units. The calculation shown in the bottom portion of the figure only includes competition between n and p emission and large yields are predicted only for $A = 67 \pm 1$.

predicted for masses 61, 64, and 67. A similar calculation for ^{32}S induced fusion on ^{25}Mg correctly reproduces the observed mass three systematics in the yield of fusion products.

A calculation not including α -particle emission is presented at the bottom of Fig. 5, demonstrating that the lighter groups of fusion products are as-

sociated with α emission. In the middle portion of Fig. 5 another nonphysical calculation is shown which allows α -particle emission but does not decrease the energy of the system when an α particle is emitted. When the excitation energy of the system is not decreased in the α -particle emission, the mass separation of the predicted fusion products is predicted to be four mass units as expected. Therefore, it is apparent that the mass three systematics observed in the fusion product yield is associated with α emission removing sufficient energy from the system so that on the average one less nucleon is emitted.

VI. SUMMARY

The mass and energy distributions for fusion products corresponding to 128.9 MeV ^{32}S on ^{12}C , ^{25}Mg , and ^{40}Ca targets has been measured with a time-of-flight spectrometer. The system was calibrated both in mass and energy by scattering various ions having masses and energies near to that of the fusion products. The heaviest fusion product group observed in all systems has a mass five units less than that of the corresponding compound system. Lighter dominant mass groups are separated by approximately three mass units. Such systematics can be understood in terms of neutron, proton, and α -particle competition in the deexcitation of the compound system and are reproduced qualitatively by particle evaporation calculations. The emission of either a neutron, proton, or α particle reduces the excitation energy of the compound system by about the same amount. On the average, then, the same total number of particles are evaporated. Therefore, when an α particle is emitted one less neutron or proton usually is evaporated resulting in the three mass unit variation in the observed yield.

ACKNOWLEDGMENTS

We wish to thank M. Blann for furnishing a copy of the code ALICE and for discussions concerning its use. The participation of P. Thieberger and S. Skorka in the early portions of this work is acknowledged.

[†]Work performed under the auspices of the Energy Research and Development Administration.

¹M. Lefort, Y. LeBeyec, and J. Péter, in *Proceedings of the International Conference on Reactions between Complex Nuclei, Nashville, Tennessee, 10-14, June 1974*, edited by R. L. Robinson, F. K. McGowan, J. B. Ball, and J. H. Hamilton (North-Holland, Amsterdam,

1974), Vol. II, p. 81 and references therein.

²K. L. Wolf, J. P. Unik, J. R. Huizenga, J. Birkelund, H. Freiesleben, and V. E. Viola, *Phys. Rev. Lett.* **33**, 1105 (1974).

³H. H. Gutbrod, F. Plasil, H. C. Britt, B. H. Erkkila, R. H. Stokes, and M. Blann, in *Proceedings of the Third International Symposium on the Physics and*

Chemistry of Fission, Rochester, 1973 (International Atomic Energy Agency, Vienna, 1974), Vol. II, p. 309.

⁴H. H. Gutbrod, W. G. Winn, and M. Blann, *Nucl. Phys. A213*, 267 (1973).

⁵A. M. Zebelman, L. Kowalski, J. Miller, K. Beg, Y. Eyal, G. Jaffe, A. Kandil, and D. Logan, *Phys. Rev. C* **10**, 200 (1974); in *Proceedings of the Third International Symposium on the Physics and Chemistry of Fission, Rochester, 1973* (see Ref. 3), Vol. II, p. 335.

⁶R. L. Robinson, H. J. Kim, J. L. C. Ford, Jr., *Phys. Rev. C* **9**, 1402 (1974); J. C. Wells, Jr., R. L. Robinson, H. J. Kim, and J. L. C. Ford, Jr., *ibid.* **11**, 879 (1975).

⁷R. Broda, M. Ishihara, B. Herskind, H. Oeschler, S. Ogaza, and H. Ryde, Niels Bohr Institute (unpublished).

⁸See, however, Refs. 6 and 7 where the cross sections for the fusion products were determined from the resulting single γ -ray spectra.

⁹T. M. Cormier, R. S. Galik, E. R. Cosman, and A. J. Lazzarini, *Nucl. Instrum. Methods* **119**, 145 (1974).

¹⁰Product of Nuclear Enterprises, San Carlos, Calif.

¹¹R. Middleton and C. T. Adams, *Nucl. Instrum. Methods* **118**, 329 (1974); and R. Middleton, in *Large Electrostatic Accelerators*, edited by D. A. Bromley (North-Holland, Amsterdam, 1974), p. 35.

¹²J. D. Garrett, H. E. Wegner, T. M. Cormier, E. R. Cosman, and A. J. Lazzarini (unpublished).

¹³Since the excitation energy of the compound system, ^{44}Ti , produced in $^{32}\text{S}+^{12}\text{C}$ is much less than for ^{32}S on ^{25}Mg or ^{40}Ca (see Table I), fewer particles should be emitted. Therefore, the heaviest product that corresponds to $^{32}\text{S}+^{12}\text{C}$ fusion should be closer in mass to the compound system than to the ^{25}Mg or ^{40}Ca targets. Such is not observed in the present experimental data (see Table I and Fig. 4). The heaviest observed product from $^{32}\text{S}+^{12}\text{C}$ fusion is the same number of mass units less than the compound system mass as for $^{32}\text{S}+^{25}\text{Mg}$ and $^{32}\text{S}+^{40}\text{Ca}$ fusion. The apparent discrepancy may result from the different kinematics for $^{32}\text{S}+^{12}\text{C}$ or perhaps from the α cluster structure of ^{12}C . The measurements for all the targets were made at the same laboratory angle at 8° . Since center-of-mass corrections are more severe for the lighter target and the angular distribution of fusion fragments corresponding to multiple neutron and proton emission should be more sharply forward peaked, the heaviest products for the $^{32}\text{S}+^{12}\text{C}$ fusion already may be lost at this angle.

¹⁴F. Plasil and M. Blann, *Phys. Rev. C* **11**, 508 (1975); see also M. Blann, *Nucl. Phys.* **80**, 223 (1966).

¹⁵V. Weisskopf and D. H. Ewing, *Phys. Rev.* **57**, 472 (1940).